HEDL-SA-2161

THE STABILITY OF γ' AND γ'' IN INCONEL 706 UNDER NEUTRON IRRADIATION

L. E. Thomas

September 2, 1980

Journal Publication
Symposium on Irradiation Phase Stability

HANFORD ENGINEERING DEVELOPMENT LABORATORY
Operated by Westinghouse Hanford Company, a subsidiary of Westinghouse Electric Corporation, under the Department of Energy Contract No. EY-76-C-14-2170

EAB

SA-2161

THE STABILITY OF γ' AND γ'' IN INCONEL 706 UNDER NEUTRON IRRADIATION*

L. E. Thomas
Hanford Engineering Development Laboratory
Richland, Washington

Inconel 706, a commercial γ'-γ'' hardenable Fe-Ni-Cr base superalloy was examined by transmission electron microscopy after neutron irradiation up to 15 x 10^{22} n/cm^2, E >0.1 MeV, at 400 to 735°C. Compared with other γ'-hardened superalloys, this alloy is exceptionally resistant to irradiation-induced swelling and creep. Phase instabilities found after irradiation include the replacement of γ'' by γ' at 400 to 500°C, and redistribution of γ' and γ'' to irradiation-induced dislocations at 550 to 650°C. These instabilities are shown to result from segregation of nickel and niobium to point defect sinks. The dislocations formed during irradiation are extrinsic Frank partial loops which grow within γ'; stacking faults produced by growth of these dislocations are identical to thin sheets of η-phase. However, the presence of η-phase as stacking faults within γ' does not accelerate replacement of γ' and γ'' by η. The γ' rather than η remains the stable phase. During either thermal aging or irradiation above 650°C, stable η forms at the expense of both γ' and γ''. In general, the behavior of this alloy under irradiation makes it attractive for nuclear energy applications requiring high strength up to 650°C.

* This work was supported by the Department of Energy.

Introduction

As part of a program to develop alloys for fast breeder reactor core applications, swelling and phase stability under high fluence neutron irradiation are being studied in a number of steels and iron-nickel base superalloys. Among these alloys, Inconel alloy 706 is a γ'-γ'' hardenable superalloy with attractive strength, fabricability, weldability and creep resistance properties. The present paper describes the stability of this alloy under neutron irradiation to 1.5×10^{23} n/cm^2, E >0.1 MeV, at 400 to 735°C.

The precipitation behavior of alloy 706, like that of the closely related alloy 718, is described extensively in published work (1-4). Age hardening in these alloys occurs by precipitation of finely-dispersed, coherent γ' and γ'' in an austenitic matrix. The γ'' phase is DO_{22}-ordered bct Ni_3Nb and forms as disk-shaped particles on {100} matrix planes, whereas the γ' is $L1_2$-ordered fcc $Ni_3(Ti,Nb,Al)$. Both phases have parallel orientation relationships with the matrix. Heat treatments used for optimum thermal stability of the γ' and γ'' produce a "compact" or "envelope" morphology in which cuboidal γ' particles are completely enclosed by γ'' disks (3). Despite the presence of both phases, however, coherency strengthening by γ'' is said to be responsible for most of the strength increase after aging (5).

During prolonged thermal aging above 650°C the creep and tensile strengths of these alloys deteriorate due to particle coarsening and replacement of the γ' and γ'' by coarse DO_{24}-ordered hcp η (nominally Ni_3Ti) and orthorhombic Ni_3Nb-δ (1,2). The "overaging" reactions accelerate rapidly with increasing temperature; γ' and γ'' are regarded as metastable with respect to η and δ. Commercially recommended heat treatments use η or δ formation at grain boundaries to limit grain growth and improve creep rupture life (1).

Previous studies of alloys 706 and 718 using nickel ion bombardment to simulate neutron irradiation showed excellent swelling resistance (6) but poor phase stability under irradiation (7). Ion bombardment at 475 to 725°C produced stable intragranular η-phase at the expense of preexisting γ' and γ''. The neutron irradiation work reported here confirms the swelling resistance of alloy 706, but gives a very different view of phase stability under irradiation.

Experimental Details

Inconel 706 was obtained as 38 mm diameter bar stock (heat no. 48C5HK) from Huntington Alloys. Table I gives the composition in weight percent according to a vendor-independent wet chemical analysis. Following the heat treatments given in Table I, specimens were machined to 3.0 mm diameter by 12.7 mm long right cylinders and irradiated in EBR-II in sodium-filled subcapsules. The subcapsules operated at constant temperatures from 400 to 650°C controlled by heat losses through an inert gas gap and calibrated by thermal expansion difference temperature monitors. Specimens examined in the present

Table I. Inconel 706 Composition (Wt.%) and Heat Treatments

Fe	Ni	Cr	Ti	Al	Nb	C	Si
37.4	41.5	16.1	1.7	0.3	2.9	0.03	0.1

Solution-Treated (ST):	1065°C/1 hr/WQ
Solution-Treated and Aged (STA):	954°C/1 hr/WQ + 843°C/3 hr/AC + 718°C/8 hr/FC to 621°C/18 hr/AC

work were irradiated to peak fluences of 5.9, 10.0 and 14.7 x 10^{22} n/cm^2, E >0.1 MeV. Table II gives the fraction of the peak fluence received by each subcapsule. Specimens irradiated to 2 x 10^{22} n/cm^2 at 427°C and 3.4 x 10^{22} n/cm^2 at 735°C were also examined.

Table II. Fraction of Peak Fluence Received by Each Constant-Temperature Subcapsule

Design Temperature (°C)	Fraction of Peak Fluence
400	0.67
427	0.84
510	0.95
538	0.89
593	1.00
650	0.99

For transmission electron microscopy (TEM), specimens were gang-sliced into 0.025 cm thick disks using a slow-speed diamond saw and jet electropolished in 10% perchloric acid, 90% butanol at 65 V. This method provides self-supporting, centrally-perforated 3 mm diameter specimens. Most examinations were performed on 100 kV and 200 kV transmission/scanning transmission electron microscopes equipped for semi-quantitative elemental analyses of microbeam-selected specimen regions by energy-dispersive X-ray (EDX) spectrometry. The void, precipitate and dislocation structures of both irradiated and unirradiated specimens were examined systematically using a standard set of diffraction conditions to image all microstructural features in a given specimen region. Dark-field images formed with various precipitate, matrix and relrod reflections near a [001] matrix orientation were used to distinguish γ' and γ'' phases and to identify thin sheet structures such as stacking faults or η-phase plates.

The EDX microanalysis capability was used in combination with selected area electron diffraction to identify η-phase particles at grain boundaries and also to determine phase compositions. EDX analyses involved positioning a 10 nm diameter electron beam probe on selected particles in specimen regions 50 nm or less in thickness and analyzing the X-rays generated. The analyses inevitably included contributions from matrix regions around the particles, but were adequate for simple phase characterizations.

Void swelling was analyzed by automated recording and data processing of void image sizes, which were measured from micrographs using a device similar to a Zeiss particle size analyzer. Specimen thicknesses were measured from stereoscopic pairs of micrographs, and the void shapes were taken into account in measuring void volume fractions.. Errors in swelling measurements are estimated as ±10% of the measured values. However, the irregular distributions of voids at low void densities probably caused a sampling uncertainty of about 100%.

Results

Preirradiation Microstructures

The STA treatment for alloy 706 produces uniformly dispersed intragranular γ' and γ'' with a mixed envelope morphology consisting of isolated γ'' disks and cuboidal γ' enclosed by γ'' disks. Some γ' nucleates on dislocations, and these particles contain internal {111} stacking faults which can be imaged

using their relrods (8). Figure 1 shows the γ' and one of the three γ" variants in $\bar{g}$ = [100] dark-field. Although the stacking faults within γ' constitute local hcp stacking within the Ll_2-ordered structure and therefore are identical to thin sheets of η-phase (9,10), the faults show no tendency to coarsen into stable η. Grain boundaries in the STA alloy contain cellular η-phase which forms during the solution and stabilization parts of the heat treatment. Electron diffraction and EDX microanalysis showed only hcp-η at grain boundaries. Although δ-phase at grain boundaries has been reported in alloy 706 with the same STA heat treatment as that in the present work (1,4), we found no δ. Difficulties in identifying δ by electron diffraction were mentioned by these same authors, and in view of their comments and the present results, the previous identifications of δ in this alloy are questionable.

In the ST condition, alloy 706 is an essentially single phase solid solution with no second phases apart from primary MC carbides.

Void Swelling

Both ST and STA alloy 706 are highly resistant to void swelling. Voids appear at fluences below 2 x 10^{22} n/cm^2, but grow little or not at all with increasing fluence. The voids are cubo-octahedra which form mainly in association with η and other structures that were present before irradiation. Locally high void concentrations and sizes occur at cellular η regions in the STA alloy, as shown in Figure 2; however, these relatively high swelling regions contribute negligibly to the total swelling, and were excluded in swelling analyses.

The analysis results given in Table III for the peak fluence of 14.7 x 10^{22} show maximum swelling of 0.1%, the same as is observed at 6 and 10 x 10^{22} n/cm^2. Void densities remain less than 1 x 10^{14} cm^{-3}, and the void sizes give no indications of void growth after 6 x 10^{22} n/cm^2. Scatter in the void density, size, and swelling results for different fluences at a given irradiation temperature probably reflects measurement uncertainties. These results indicate that void swelling in STA Inconel 706 ceases after 6 x 10^{22} n/cm^2.

Table III. Void Swelling in STA Inconel 706

Irradiation Temperature (°C)	Void Density (Voids/cm^3)			Mean Size* (nm)			Void Swelling (%)		
	Peak Fluence (x 10^{22} n/cm^2)								
	6	10	14	6	10	14	6	10	14
400	-	-	5.4 x 10^{13}	-	-	26	-	-	0.04
427	3.0 x 10^{12}	1.6 x 10^{14}	4.5 x 10^{13}	12	25	28	<0.01	0.10	0.04
482	-	-	2.6 x 10^{13}	-	-	43	-	-	0.09
510	2.4 x 10^{13}	1.3 x 10^{13}	1.2 x 10^{13}	41	30	45	0.09	0.01	0.05
538	-	-	1.1 x 10^{13}	-	-	42	-	-	0.06
593	-	1.7 x 10^{12}	-	-	69	-	-	0.02	-
650	No Voids			No Voids			No Voids		

* Equivalent sphere diameter.

Specimens irradiated at 650°C contain no voids, but do show small (5 nm diameter) features thought to be bubbles of transmutation-induced helium. Helium bubbles were found only at (and above) 650°C, and are distinguished from voids by their size and occurrence along dislocations, grain boundaries and η-phase particles. Figure 3 shows these bubbles associated with the

dislocations bounding stacking fault η-phase plates.

Phase Stability

Neutron-irradiated alloy 706 shows several complex and interrelated microstructural changes involving phase stability. These include the dissolution of γ" at low fluences and temperatures, formation of incipient η-phase as γ'-coated stacking faults produced by growth of irradiation-induced Frank dislocation loops, γ' and γ" redistribution to point defect sinks, precipitation from solution, particle coarsening and transformation of γ' and γ" to stable η. Figure 4 shows the irradiation temperatures at which these effects occur, and the following paragraphs describe the observations in more detail.

The Disappearance of γ". During irradiation at 400 to 510°C, the γ" produced by STA treatment dissolves and is replaced by γ' which forms on irradiation-induced dislocation loops. Very little γ" remains in STA specimens after 2×10^{22} n/cm^2 at 430°C, and there is none after 4×10^{22} n/cm^2. The γ" disappearance at low irradiation temperatures, as well as enhanced γ" precipitation and coarsening at 650°C, is apparent in selected area diffraction patterns from the [001] matrix orientation, in Figure 5. In unirradiated specimens the γ" reflections appear streaked along <100> directions due to the shape and limited thickness of the γ" particles. These reflections disappear completely after irradiation at 400°C, and are weak and diffuse at 510°C, indicating a decrease in γ" volume fraction and changes in particle shape. At 650°C, the γ" reflections are more intense and less extended, indicating coarsening. However, the γ' diffraction spots remain relatively unchanged at all irradiation temperatures. Also, no further change in the γ" reflections occurs with increasing fluence after 6×10^{22} n/cm^2.

To confirm that the γ" disappearance is due to irradiation, an unirradiated STA specimen was thermally aged for 15,000 hours at 430°C. This treatment produced no detectable change in the original γ' or γ", in contrast to the marked changes in both of these phases after a few thousand hours in reactor.

In ST specimens, γ', but not γ", forms during irradiation below 510°C. Both γ' and γ" precipitate from solution during irradiation at 510 to 650°C.

Irradiation-Induced Dislocations, Stacking Faults and Incipient η-Phase. Irradiation-induced dislocations in alloy 706 consist of Frank faulted loops (a/3<111> Burgers vectors) that form entirely within γ' and grow slowly without unfaulting. In most other fcc alloys under irradiation, Frank loops form in the alloy matrix and unfault at relatively low fluences by interacting with other dislocations. Diffraction contrast experiments on the irradiation-induced Frank loops in alloy 706 showed that these dislocations all formed from interstitials, i.e., the faults are extrinsic type, as is usually the case in irradiated fcc alloys. Each extrinsic stacking fault within γ' constitutes seven planes of hcp stacking in the $L1_2$-ordered structure (9). Consequently, the dislocations are identical to thin sheets of η-phase. However, this "incipient" η exists only by its identity as faulted γ', and at most irradiation temperatures shows no coarsening at the expense of its γ' coating.

The incipient η formed during irradiation gives prominent <111> relrods which extend completely between all matrix reflections, indicating that the faults are about an atom plane in thickness. Faults on all four {111} planes in an STA specimen irradiated at 510°C are imaged together with dislocations in Figure 6 by using the [200] matrix reflection and its satellite <111> relrod spots near a [001] matrix orientation. Dark-field micrographs taken with $\bar{g}$ = [100] and $\bar{g}$ = [1 1/2 0] (in fcc matrix notation), respectively, show all the γ' plus one γ" variant, and a single γ" variant from the same specimen

area. Comparison of these micrographs and the γ'-γ" structures before irradiation (Figure 1) shows that γ'-coated stacking faults extend entirely through the original γ' particles, distorting the particles in apparent shape and size. The presence of <111> relrod satellites around γ' superlattice reflections in the inset diffraction pattern in Figure 6 also indicates that the stacking faults are inside the γ' particles. Matrix and γ' fundamental reflections superimpose, so that the presence of relrod satellites around the fundamental diffraction spots does not mean that thin {111} sheet structures exist in the alloy matrix.

γ'-γ" Redistribution. Figure 6 also shows that the original γ' particles in STA material are redistributed onto Frank loops, and that γ' has precipitated at voids and Frank loops in the matrix. In addition, the relatively few remaining γ" particles appear changed in shape and location; the envelope morphology of γ" on γ' particles is lost.

A similar set of γ', γ" and <111> relrod micrographs from an ST specimen irradiated at 510°C, in Figure 7, shows extensive precipitation of γ' and γ" from solution. Enhanced γ' precipitation occurs at the irradiation-induced dislocations, and regions around the dislocations are denuded of γ" particles. The denuding of γ", but not γ', around dislocations suggests that elemental components of the Ni_3Nb-γ" phase are preferentially attracted to point defect sinks and precipitated as γ'. To determine which elements are segregated at the dislocations, individual particles of the irradiation-induced γ' were examined by energy-dispersive X-ray microanalysis. These analyses showed that the γ' on dislocations is highly enriched in niobium and contains relatively little titanium. Thus, the disappearance of γ" during irradiation at 400 to 500°C can be attributed to radiation-induced segregation of niobium to point defect sinks, and its subsequent reprecipitation as γ'. Niobium should be an oversized atom in this alloy (11), and its observed concentration at point defect sinks is especially noteworthy because it violates the "rule" that oversized solutes move away from sinks (12).

η-Phase Formation. Since γ' is regarded as metastable with respect to η-phase, the presence of incipient η as stacking faults in γ' raises the question of whether neutron irradiation accelerates the γ'→η transformation. Electron diffraction patterns from specimens irradiated up to 10×10^{22} n/cm^2 at 400 to 600°C show <111> relrods extending completely between matrix reflections and no diffraction maxima due to η-phase. Also, the γ' reflection intensities are undiminished after irradiation. These observations indicate that γ' rather than η remains the stable phase during neutron irradiation.

After 13,000 hour irradiation (10×10^{22} n/cm^2) at 650°C extended {111} stacking fault structures develop within grains, and cellular η grows at grain boundaries in STA specimens. The extended {111} stacking faults do not appear coated with γ', although γ'-coated faults are still present, as shown in Figure 8. Also, coarsened and redistributed γ' and γ" remain, and diffraction spot intensities indicate little loss in γ', γ" volume fraction after irradiation. Even at this fluence the η is too thin to produce distinct intensity maxima in diffraction patterns. As shown in Figure 9, <111> relrods extend completely between fundamental reflections, and partially between γ' superlattice reflections, but show no intensity maxima from the η-phase. However, the relrods do produce diffraction "spots" on [111] zone axis patterns that could be misinterpreted as η reflections.

At temperatures above 650°C, Widmanstätten η-phase forms rapidly as coarse plates both in irradiated and thermally aged alloy 706. The η forms at the expense of both γ' and γ", and EDX microanalyses of large η plates in both irradiated and unirradiated specimens yield a characteristic formula $Ni_3(Ti_{0.5}Nb_{0.4}Al_{0.1})$ for this phase which is usually regarded as stoichiometric Ni_3Ti.

The γ' + γ"→η transformation is complete after 3.4×10^{22} n/cm^2 (irradiation time of 6,700 hours) at 735°C, as shown in Figure 10. Comparison with a

thermal control specimen aged for 7,000 hours at 735°C indicates that the transformation to η may be slightly faster during irradiation. Areas containing coarse γ' and γ" remain after the thermal aging treatment but not after irradiation. However, the differences in temperatures needed to produce these microstructural differences are small enough (less than 50°C) to fall within the temperature uncertainties of the irradiation experiments. Thus, neutron irradiation accelerates the transformation of γ' and γ" to η slightly, if at all. No δ-phase forms during thermal aging or irradiation in alloy 706.

Discussion

Swelling Behavior

Compared with other Fe-Ni-Cr based superalloys, alloy 706 shows exceptional swelling resistance and phase stability behavior. For example, the well-known γ' hardenable superalloy, Nimonic PE16, with about the same base composition as alloy 706 but with Ti and Al as hardeners instead of Ti and Nb, shows no saturation of swelling during neutron irradiation. After 10 x 10^{22} n/cm^2 in the same irradiation test described in this paper, STA Nimonic PE16 swelled about twenty times as much as STA alloy 706. Ternary Fe-Ni-Cr alloys show low swelling near this base composition (13,14) but exhibit continued void growth like Nimonic PE16.

The cause of the swelling resistance in alloy 706 is not clear, but appears related to the formation of irradiation-induced dislocations within γ'. In STA 706, regions of locally high, sustained swelling were found associated with cellular η which formed at grain boundaries before irradiation. The dislocation structures in these regions consisted of Frank and prismatic loops with no γ' coatings, and EDX microanalyses showed that the compositions of the γ'-free matrix were the same in cellular and non-cellular regions. Thus, the inhibited swelling in alloy 706 is related to microstructure rather than to composition.

To grow at the γ'-matrix interface, irradiation-induced dislocations in γ' require Ni and Nb, Ti or Al - as well as a net flux of interstitial atoms. EDX microanalyses showed that the irradiation-induced γ' on the dislocations contains mainly Ni and Nb, implying that both of these solutes segregate strongly to point defect sinks during irradiation. The irradiation-induced γ' forms initially by precipitation from solution and by redistribution of the original γ' and γ" formed by STA treatment. During irradiation, however, the γ' and γ" which form at sinks are continuously redistributed. Dissolution of γ' and γ" particles and the diffusional transport of solute to point defect sinks can therefore be seen as the limiting steps in dislocation growth and consequent swelling.

On the other hand, the chemical potentials of the irradiation-induced vacancies and interstitials may be large enough to cause the dislocations to climb outside the γ' structure. If this is the case, atomic order at the dislocation must be restored by rearrangement of the adjacent γ', since the dislocations exist entirely within the γ' phase. Another possibility to be considered is that dislocations within γ' grow slowly because they have no strong bias for preferential absorption of interstitials. The interfacial strains between γ' particles and the matrix in Inconel 706 may reduce the strain field of interstitial Frank loops growing within the γ' so that their preference for interstitial atoms is decreased. This could occur if the irradiation-induced γ' has a smaller lattice parameter than the matrix. However, lattice parameter measurements from electron diffraction patterns do not show significant differences in d-spacings between the matrix and γ'.

Dislocation loop growth was not measured in the present work, but appears to proceed very slowly after 6 x 10^{22} n/cm^2. This indicates slow irradiation creep in alloy 706 as well as low swelling. However, continued growth of the dislocations indicates that excess vacancies are accumulating during irradiation. Whether the vacancies are trapped by solutes, stored by the γ' structures or are simply present in small concentrations in accord with the observed slow growth of the dislocations is unclear. It is clear, however, that these excess vacancies do not produce significant void swelling.

γ'-γ" Stability Under Irradiation

Until recently, precipitate stability in γ'-containing alloys under irradiation was thought to be controlled by recoil dissolution (disordering and removal of atoms by energetic cascades) and radiation-enhanced diffusion. The Nelson-Hudson-Mazey (NHM) model (15) based on these concepts predicted γ' dissolution (15) at low irradiation temperatures and the establishment of an equilibrium γ' size independent of the initial particle size. The model was based on experimental observations in ion and neutron irradiated Nimonic PE16 and similar alloys (16).

Subsequent neutron irradiation work has not supported either the NHM model or the experimental observations on which it is based. For example, in Nimonic PE16 irradiated to a peak fluence of 10 x 10^{22} n/cm^2 at 430 to 650°C, Gelles (17,18) found no evidence of γ' particle dissolution or an equilibrium γ' size. Gelles also showed that the γ' precipitate behavior under neutron irradiation is controlled by coarsening (Ostwald ripening), and γ' redistribution to point defect sinks. The coarsening is enhanced by about four orders of magnitude at 425°C due to irradiation-enhanced diffusion, and is similar to thermal coarsening at 650°C.

Radiation-enhanced precipitation from solution, precipitate redistribution due to solute segregation at point defect sinks, and enhanced precipitation from solution also account for the γ' stability behavior observed in neutron irradiated alloy 706. Formation of a point defect sink structure that consists mainly of interstitial-type Frank loops in γ' is an additional important factor in the γ' behavior. However, the disappearance of γ" during irradiation at 400 to 500°C, i.e., at temperatures where γ' and γ" are stable under thermal aging, superficially resembles the particle dissolution predicted by the NHM model.

The present observations indicate that γ" dissolution occurs by radiation-induced segregation of nickel and niobium to Frank loops, and reprecipitation of these elements as γ'. The observations include γ" denuding around γ'-coated Frank loops in ST specimens, EDX microanalyses showing that the γ' on loops is enriched in niobium, and the redistribution of γ" as well as γ' to Frank loops during irradiations above 500°C. Below 500°C, no γ" forms in ST specimens during irradiation and γ', but not γ", precipitates during thermal aging. Thus, γ" may be thermodynamically unstable below 500°C. Nevertheless, the possibility that irradiation-induced formation of Ni_3Nb-γ' at the expense of preexisting γ" is an example of altered phase stability cannot be excluded on present evidence.

In previous work on nickel ion bombarded alloys 706 and 718, Bell and coworkers (7) reported that the γ' and γ" dissolved and were replaced by stable η-phase at irradiation temperatures from 475 to 725°C. The η-phase consisted of thin plates on {111} habit planes, and was identified by the observation that the η plates produce relrod intersections which appear as spots consistent with η-phase in diffraction patterns taken at a [111] matrix zone axis.

The η formed by ion bombardment appears similar to the γ'-coated η found after neutron irradiation. However, the diffraction evidence cited in the ion bombardment study does not prove the phase identity. As shown in Figure 9, any structure which gives <111> relrods extending completely between matrix spots will produce extra spots on [111] zone axis diffraction patterns because of relrods extending from upper and lower layers of the reciprocal lattice. The presence or absence of diffraction maxima along the relrods can be determined from [011] zone axis patterns showing two sets of <111> relrods in the plane of the diffraction pattern.

A possible explanation for the apparent lack of γ' stability in ion bombarded alloy 706 is that the γ' redistributed as faulted dislocation loops during ion irradiation may not have enough time to coarsen as stable γ'. The

ion irradiations achieve the same number of atomic displacements in a few hours as neutron irradiations do in a few thousand hours. Higher damage rates allow irradiation-induced particle dissolution processes to compete more effectively with thermal reordering, so that the apparent disappearance of γ' and γ'' under ion bombardment is a kinetic effect. Under neutron irradiation, γ' and γ'' clearly remain stable up to temperatures where thermally-induced η formation occurs.

Conclusions

Compared with other iron-nickel based superalloys, alloy 706 shows exceptional swelling resistance and unusual phase stability behavior during neutron irradiation. The γ' and γ'' strengthening phases are thermodynamically stable up to 650°C where they coarsen and are replaced by hcp η-phase. Both γ' and γ'' are redistributed by radiation-induced flow of Ni and Nb to point defect sinks (mainly dislocation loops) and the γ'' disappears in favor of Nb-rich γ' during irradiation below 500°C. Incipient η-phase forms as stacking faults within γ' at all temperatures from 400 to 650°C. However, the γ', $\gamma'' \rightarrow \eta$ transformation is accelerated only slightly by irradiation. Overall, the resistance to irradiation-induced swelling and creep, and maintained stability of the strengthening phases during high fluence neutron irradiation at 400 to 650°C, make this alloy an attractive candidate for fast breeder reactor core components.

References

1. L. Rémy, J. Laniesse and H. Aubert, "Precipitation Behavior and Creep Rupture of 706 Type Alloys," Materials Science and Engineering, 38 (1979) pp. 227-239.

2. D. F. Paulonis, J. M. Oblak and D. S. Duvall, "Precipitation in Nickel Base Alloy 718," Trans. ASM, 62 (1969) pp. 611-622.

3. R. Cozar and A. Pineau, "Morphology of γ' and γ'' Precipitates and Thermal Stability of Inconel 718 Type Alloys," Met. Trans., 4 (1973) pp. 47-59.

4. J. H. Moll, G. N. Maniar and D. R. Muzyka, "The Microstructure of 706, A New Fe-Ni Base Superalloy," Met. Trans., 2 (1971), pp. 2143-2160.

5. J. M. Oblak, D. F. Paulonis and D. S. Duvall, "Coherency Strengthening in Ni Base Alloys Hardened by DO_{22} γ'' Precipitates," Met. Trans., 5 (1974) pp. 143-153.

6. W. G. Johnson, J. H. Rosolowski, A. M. Turkalo and T. Lauritzen, "An Experimental Survey of Swelling in Commercial Fe-Cr-Ni Alloys Bombarded with 5 MeV Ni Ions," Journal of Nuclear Materials, 54 (1974), pp. 24-40.

7. W. L. Bell, T. Lauritzen, E. S. Darlin and R. W. Warner, "Microstructural Changes in Ion Irradiated Commercial Alloys," pp. 353-369 in Irradiation Effects on the Microstructure and Properties of Metals, ASTM STP 611, ASTM, Philadelphia, PA, 1976.

8. C. W. Allen and P. R. Okamoto, "An Imaging Technique in Transmission Electron Microscopy Utilizing Diffraction Fine Structure," Physica Status Solidi (a) 36 (1976) pp. 107-116.

9. J. M. Oblak, W. A. Owczarski and B. A. Kear, "Heterogeneous Precipitation of Metastable γ'-Ni_3Ti in a Nickel Base Alloy," Acta Met., 19 (1971) pp. 355-363.

10. D. Raynor, "Dislocation Precipitation in γ'-Forming Steels," Metal Science Journal, 5 (1971) pp. 161-165.

11. A. W. Denham and J. M. Silcock, "Precipitation of Fe_2Nb in a 16 wt. % Ni 16 wt. % Cr Steel and the Effect of Mn and Si Additions," Journal of the Iron and Steel Institute, 207 (1969) pp. 585-592.

12. P. R. Okamoto and L. E. Rehn, "Radiation-Induced Segregation in Binary and Ternary Alloys," Journal of Nuclear Materials, 83 (1979) pp. 2-23.

13. J. F. Bates and W. G. Johnston, "Effects of Alloy Composition on Void Swelling," in Radiation Effects in Breeder Reactor Structural Materials, M. L. Bleiberg, ed.; AIME, New York, NY, 1977.

14. W. G. Johnston, T. Lauritzen, J. H. Rosolowski and A. M. Turkalo, "The Effect of Metallurgical Variables on Void Swelling," in Radiation Damage in Metals, ASM, Cleveland, OH (1976) pp. 227- .

15. R. S. Nelson, J. A. Hudson and D. J. Mazey, "The Stability of Precipitates in an Irradiation Environment," Journal of Nuclear Materials, 44 (1972) pp. 318-330.

16. J. A. Hudson, "Structural Stability During Irradiation," Journal of the British Nuclear Energy Society, 14 (1975) pp. 127-136.

17. D. S. Gelles, "An Example of Precipitate Stability in Reactor Irradiated Nimonic PE16," in Effects of Radiation on Structural Materials, ASTM STP 683, ASTM, Philadelphia, PA, 1979.

18. D. S. Gelles, "Gamma Prime Coarsening and Redistribution in Nimonic PE16," in Tenth International Symposium on Effects of Radiation on Materials, ASTM, Philadelphia, PA, 1980.

FIGURE CAPTIONS

1. γ'-γ'' microstructure of unirradiated STA 706. $\bar{g}$ = [100] dark-field micrograph shows all γ' and one of the three γ'' variants. γ' particles formed on dislocations contain {111} stacking faults.

2. Voids in STA 706. Cellular η-phase region at grain boundary shows locally high swelling after 8.4×10^{22} n/cm^2 at 427°C.

3. Helium bubbles at stair rod and Frank partial dislocations bounding stacking fault η-phase in STA 706 after 14.6×10^{22} n/cm^2 at 650°C.

4. Stability behavior in irradiated alloy 706 at fluences from 2 to 15×10^{22} n/cm^2.

5. [001] selected area diffraction patterns from STA alloy 706 showing γ'' dissolution during irradiation at 400 to 510°C. Also showing enhanced γ'' precipitation and coarsening at 650°C. γ' remains stable during irradiation.

6. Selectively imaged γ', γ'' and stacking fault (relrod image) microstructures in the same area of neutron irradiated STA alloy 706 after 5.7×10^{22} n/cm^2 at 510°C. Inset diffraction pattern shows reflections used for imaging. The γ' particles are distorted by internal faulting and γ' redistribution to Frank partial dislocations bounding the faults.

7. γ',γ'', <111> relrod and void microstructures in the same area of irradiated ST 706 after 5.7×10^{22} n/cm^2 at 510°C. Enhanced γ' precipitation at dislocations occurs at the expense of surrounding γ''.

8. η-phase, γ' and γ'' in STA alloy 706 after 10×10^{22} n/cm^2 (13,000 hours in reactor) at 650°C. Transformation of γ' and γ'' to Widmanstätten η is sluggish at 650°C in reactor.

9. [011] selected area electron diffraction pattern from STA 706 after 10×10^{22} n/cm^2 (13,000 hour irradiation) at 650°C, showing extended <111> relrods but no distinct diffraction maxima from η-phase. Extra spots (arrowed) on [111] zone axis pattern (b) are due to <111> relrods extending from upper and lower reciprocal lattice layers as shown in (c). These spots do not establish the presence of η.

10. Widmanstätten η-phase formed from γ' and γ'' in STA Inconel 706.
(a) Neutron irradiated to 3.4×10^{22} n/cm^2 (6,700 hours) at 735°C.
(b) Thermally aged 7,000 hours at 735°C.

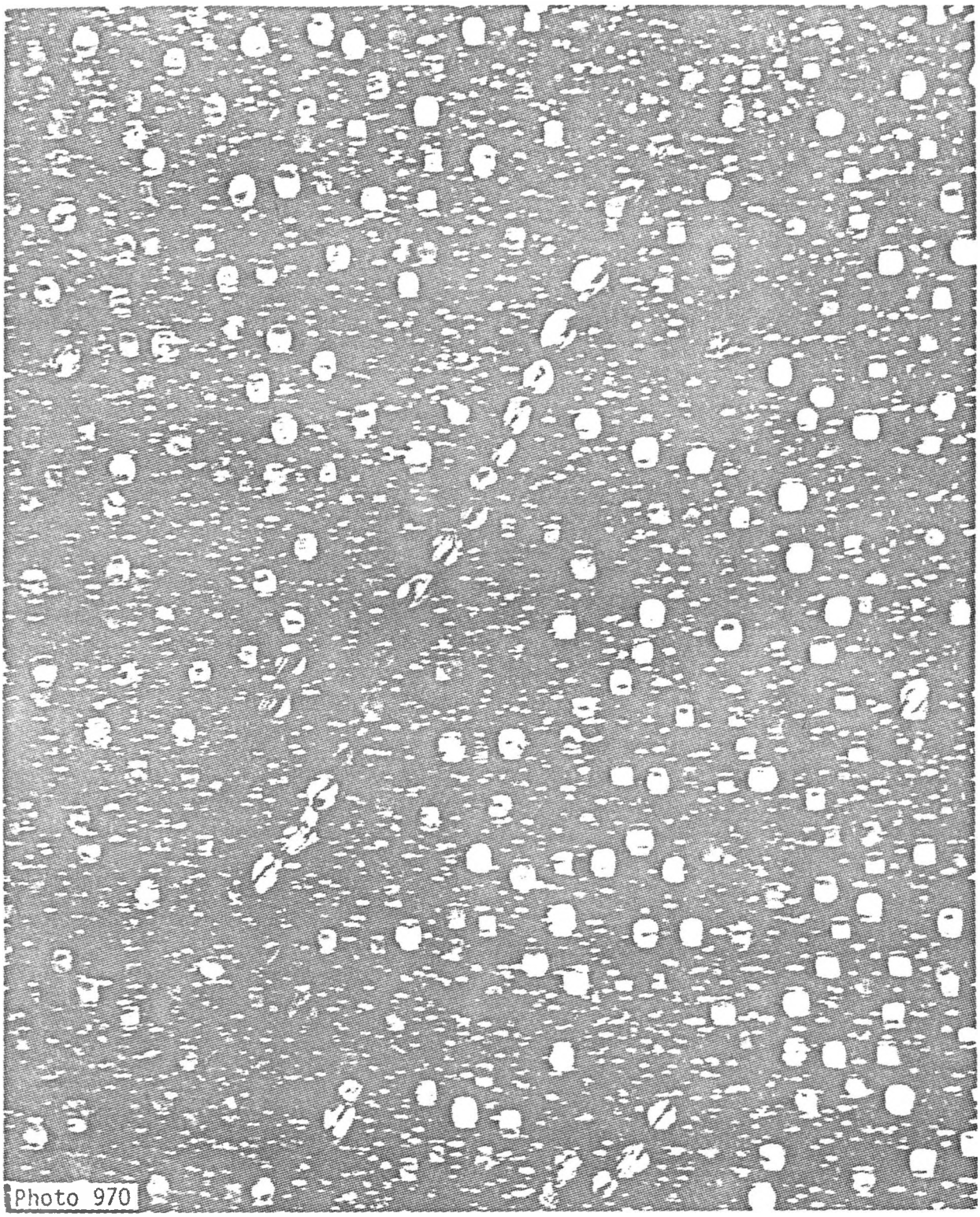

Initial γ'-γ" Microstructure of STA Inconel 706 (Before Irradiation)

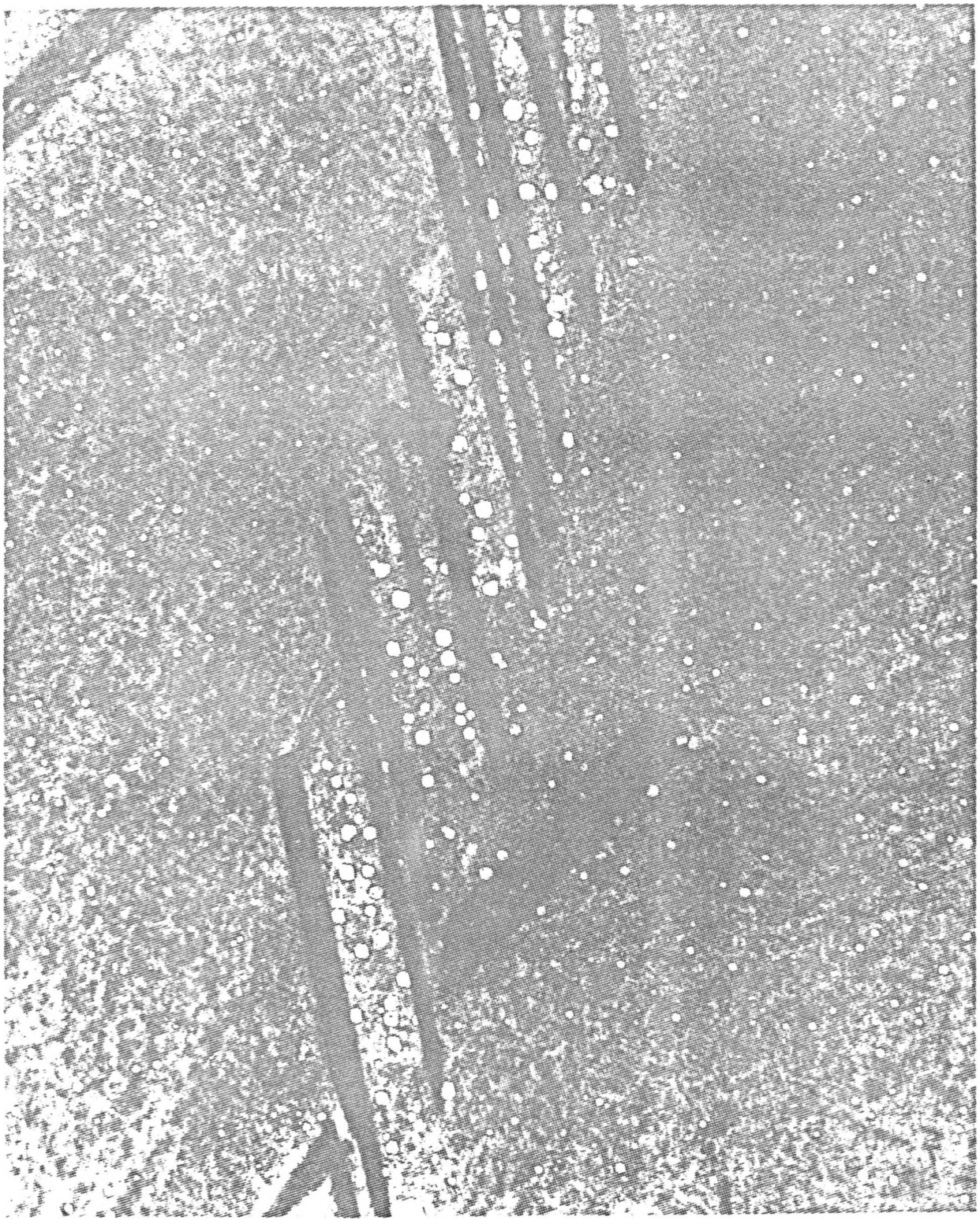

Z-phase region at grain boundary showing relatively high swelling after 8 x 10^{22} n/cm^2 at 427°C.

Fig 2

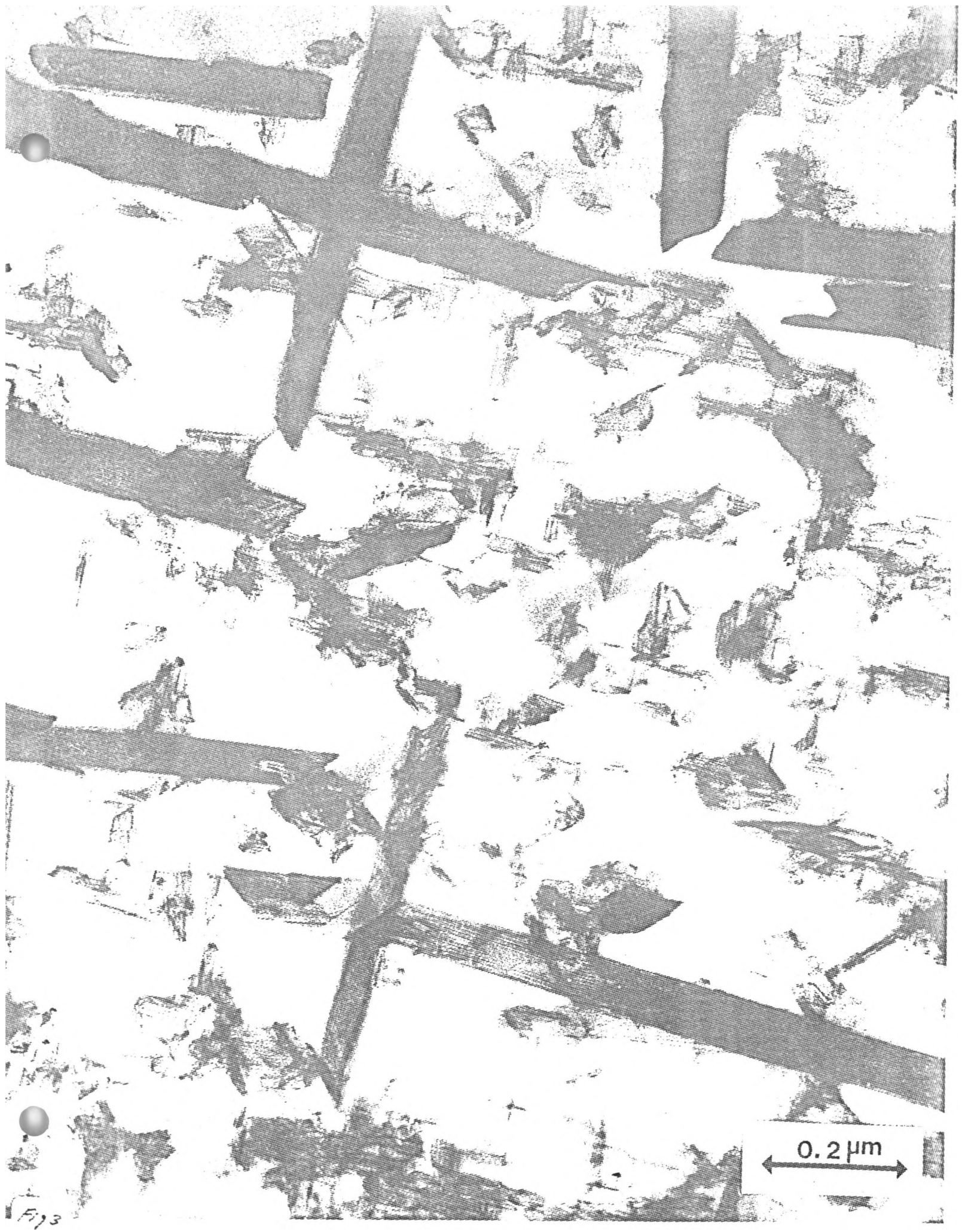

Fig 3

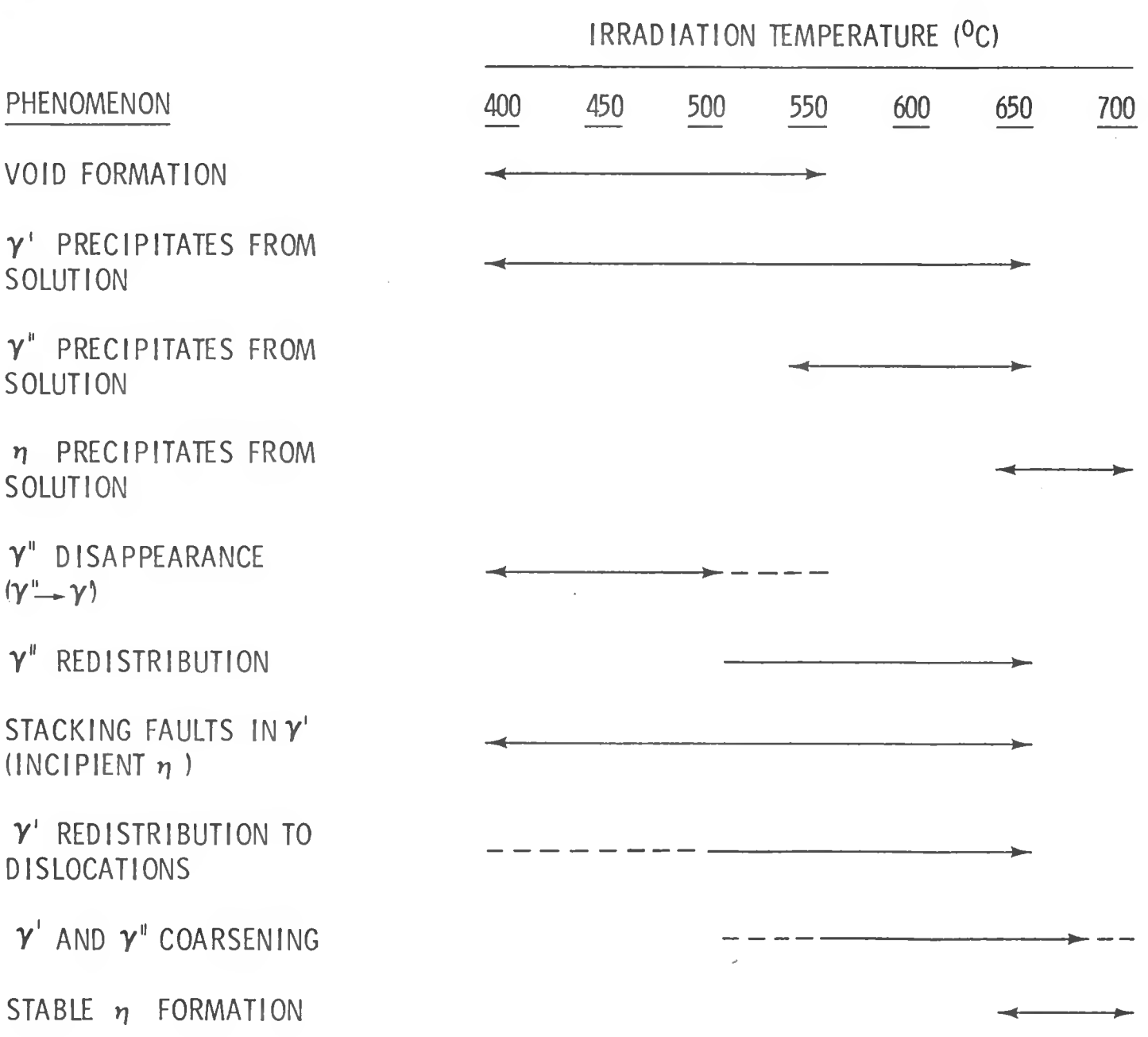

HEDL 7910-273.3

Fig 4

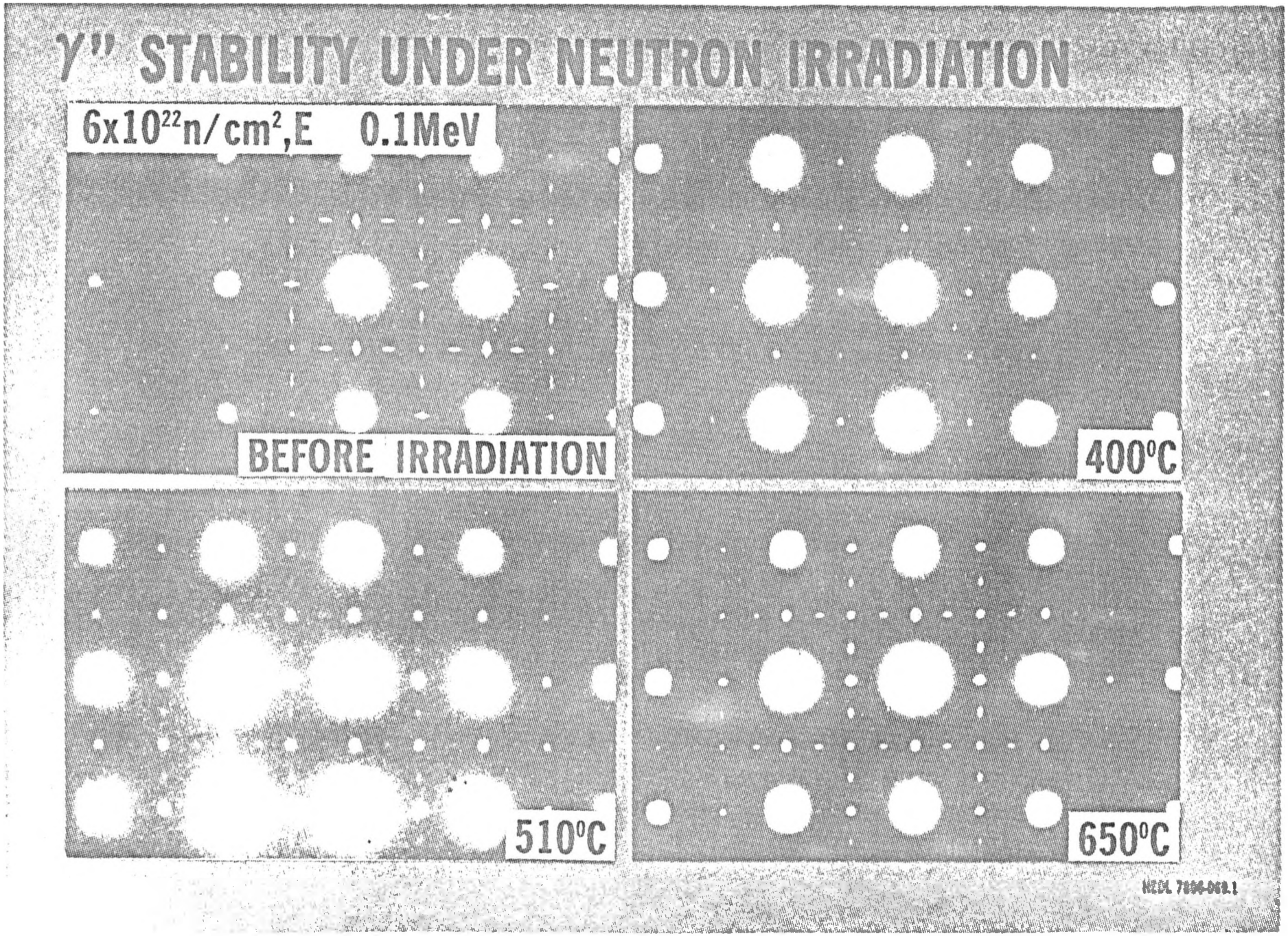
γ'' STABILITY UNDER NEUTRON IRRADIATION
6x10²²n/cm², E 0.1MeV
BEFORE IRRADIATION
400°C
510°C
650°C

STA INCONEL 706

6×10^{22} n/cm^2, 510°C

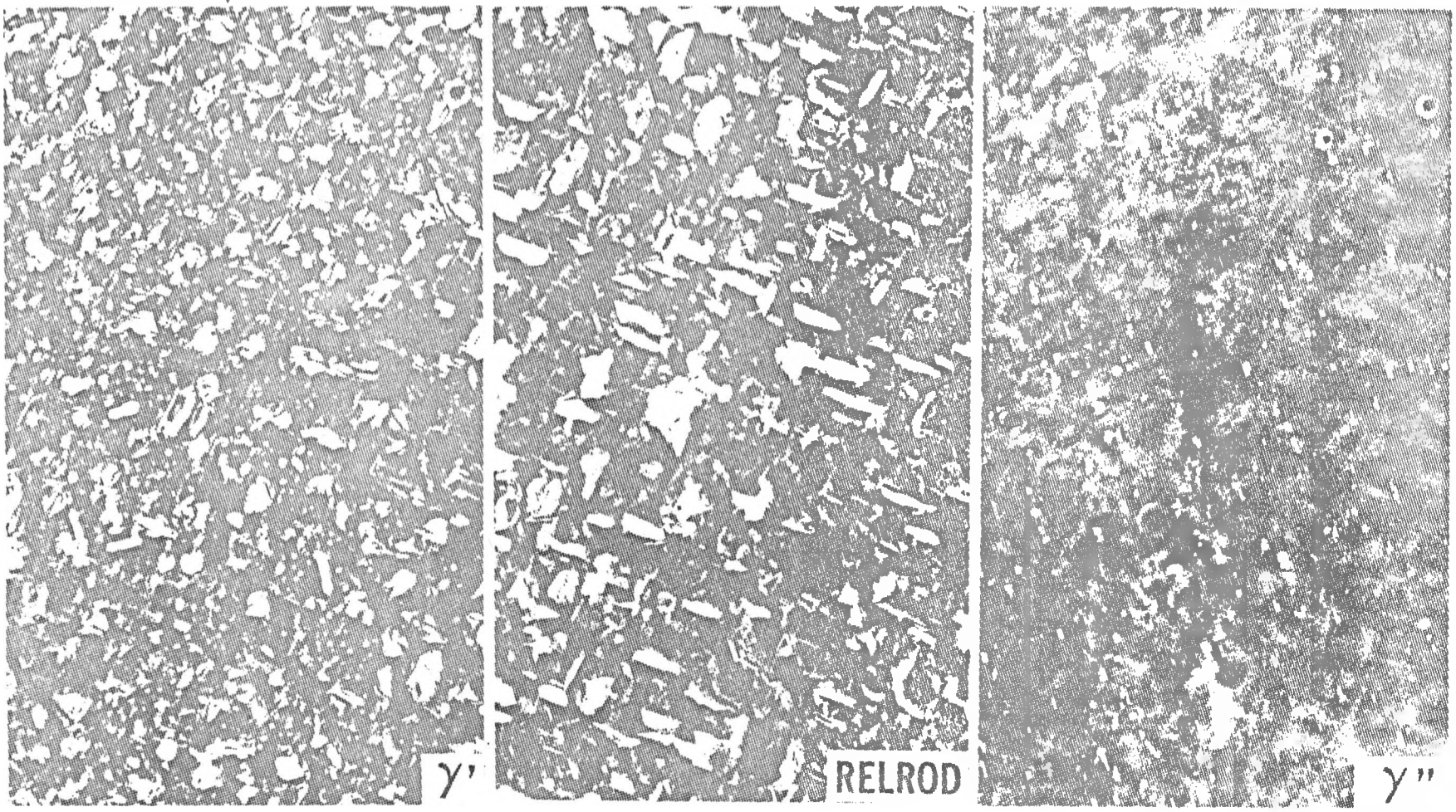

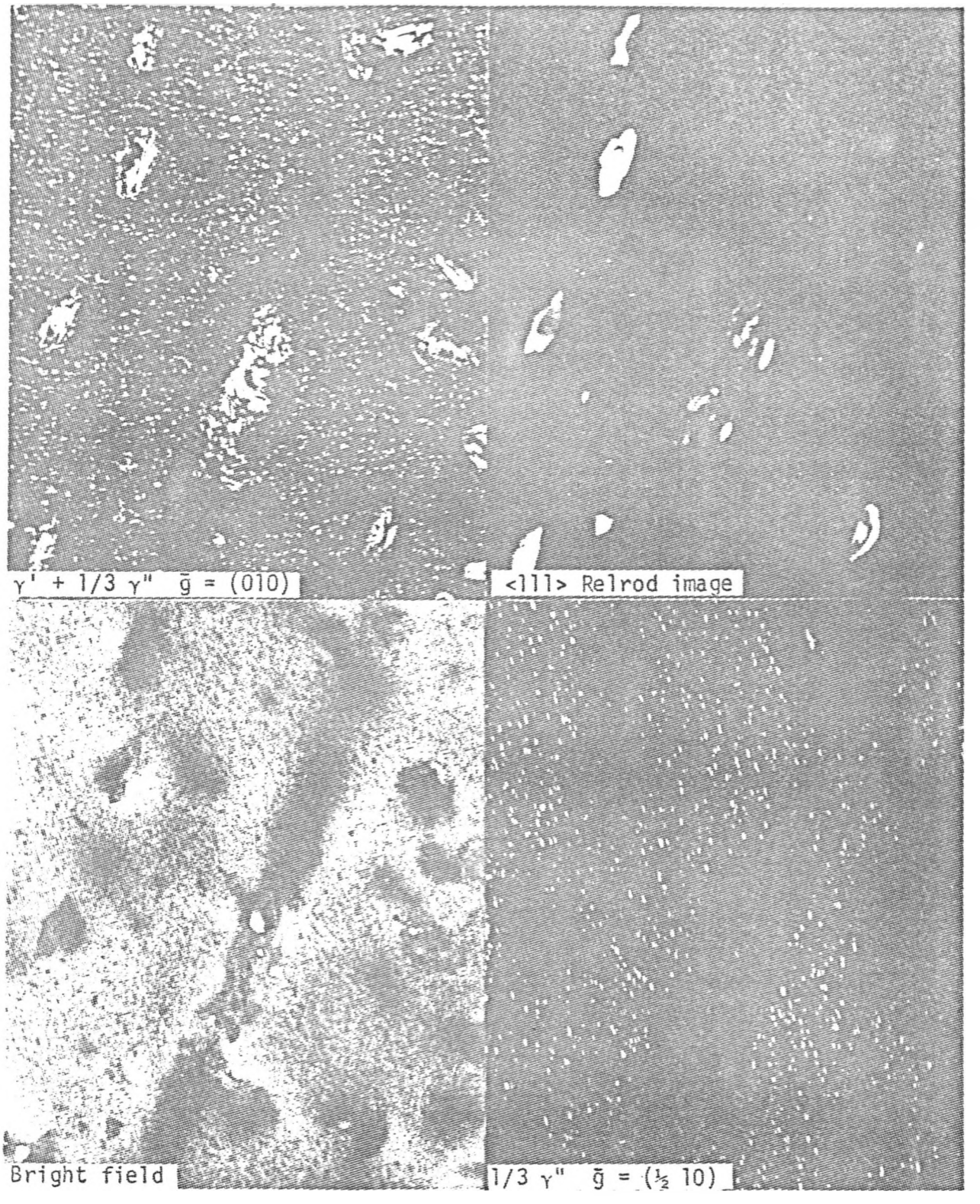

γ',γ" Dislocation and Void Microstructures in the Same Area of Neutron Irradiated ST Inconel 706

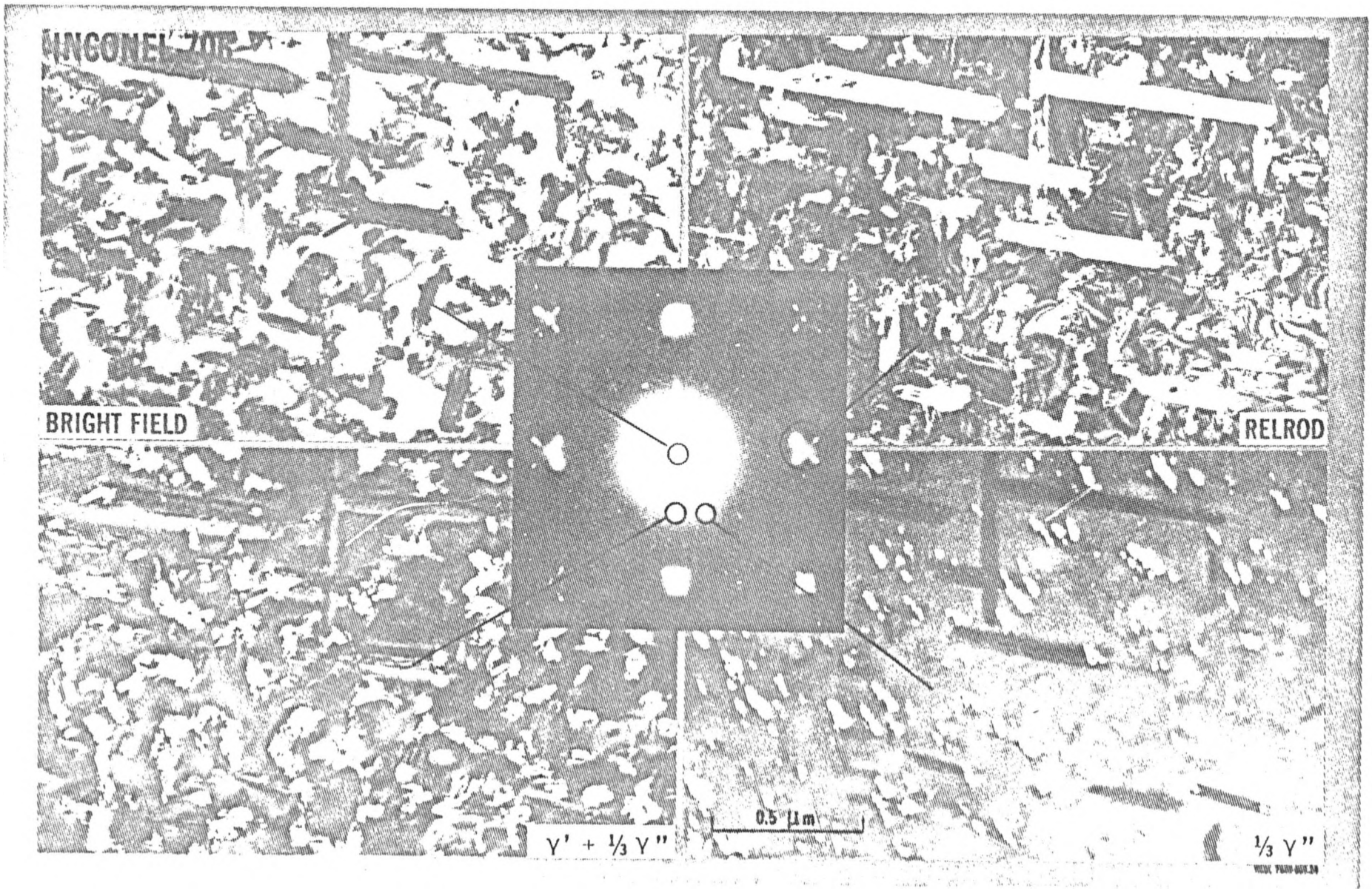

Fig

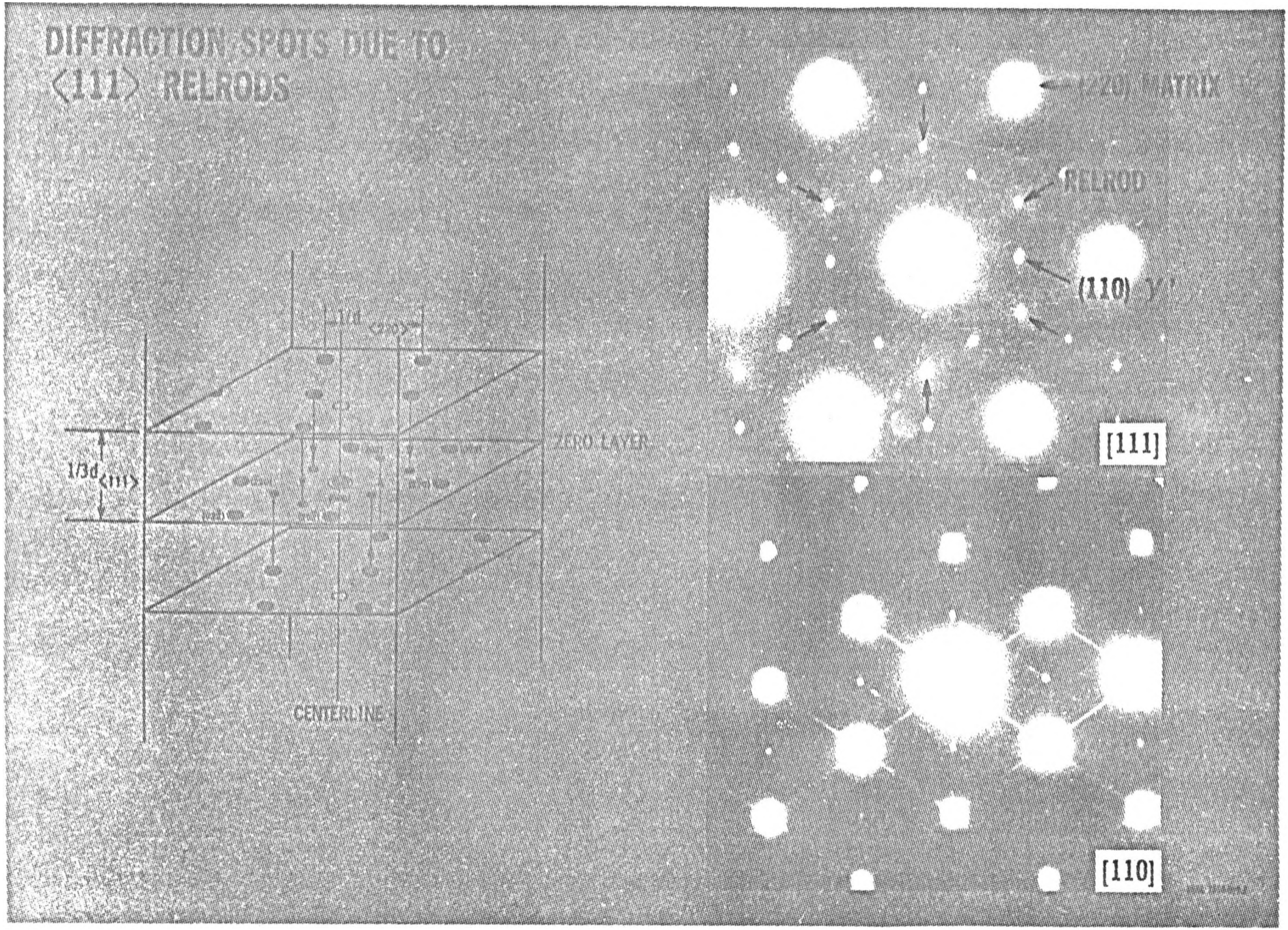
DIFFRACTION SPOTS DUE TO
<111> RELRODS
1/d <110>
1/3d <111>
ZERO LAYER
CENTERLINE
MATRIX
RELROD
(110)
[111]
[110]

Widmanstätten η phase in Neutron Irradiated STA Inconel 706 After 3.4×10^{22} n/cm^2 (E >0.1 MeV) (6,700 Hours) at 735°C.

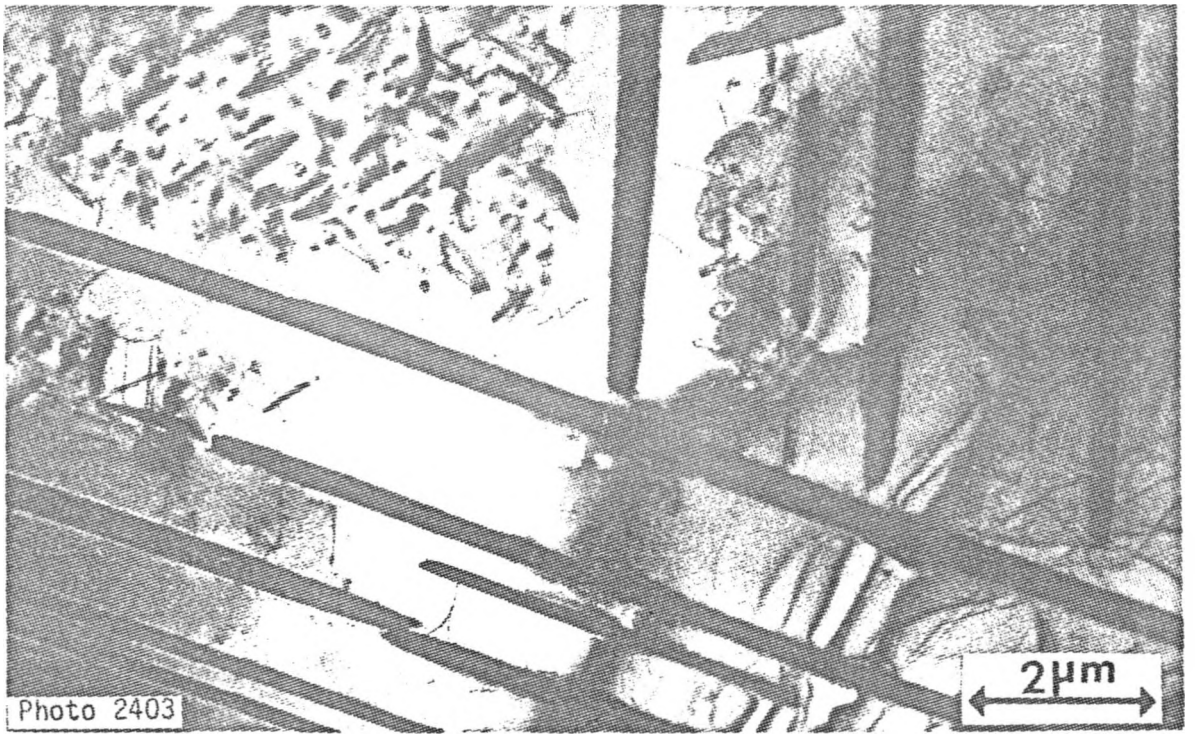

Thermally-Aged Inconel 706 Showing Widmanstätten η Phase and Undissolved γ' and γ" After 7,000 Hours at 735°C.